MSFC-191 PAPER

ANALYSIS OF LUNAR SURFACE CHARGING FOR A CANDIDATE SPACECRAFT USING NASCAP-2K

Linda PARKER[1], Dr. Joseph MINOW[2], and William BLACKWELL, Jr.[1]

[1]*Jacobs Technology, ESTS Group, EV13, Huntsville, AL 35806 (USA)*

[2]*NASA, Marshall Space Flight Center, EV13, Huntsville, AL 35812 (USA)*

ABSTRACT : The characterization of the electromagnetic interaction for a spacecraft in the lunar environment, and identification of viable charging mitigation strategies, is a critical lunar mission design task, as spacecraft charging has important implications both for science applications and for astronaut safety. To that end, we have performed surface charging calculations of a candidate lunar spacecraft for lunar orbiting and lunar landing missions. We construct a model of the spacecraft with candidate materials having appropriate electrical properties using Object Toolkit and perform the spacecraft charging analysis using Nascap-2k, the NASA/AFRL sponsored spacecraft charging analysis tool. We use nominal and atypical lunar environments appropriate for lunar orbiting and lunar landing missions to establish current collection of lunar ions and electrons. In addition, we include a geostationary orbit case to demonstrate a bounding example of extreme (negative) charging of a lunar spacecraft in the geostationary orbit environment. Results from the charging analysis demonstrate that minimal differential potentials (and resulting threat of electrostatic discharge) occur when the spacecraft is constructed entirely of conducting materials, as expected. We compare charging results to data taken during previous lunar orbiting or lunar flyby spacecraft missions.

1 - INTRODUCTION

Development of space systems for reliabile operation in lunar environments will necessarily need to consider spacecraft charging. It has been known since the first exploration of the Moon by robotic and manned spacecraft that the lunar dayside charges to a few tens of volts where the photoelectron current is the dominant charging process [1, 2] and negative nightside potentials develop due to the preferential collection of hot electrons that penetrate the plasma wake [3]. The early observations and theoretical studies are consistent with the more recent results from the Lunar Prospector spacecraft which demonstrate positive lunar surface potentials in the daylit hemisphere and negative surface potentials reported on the order of a few hundred volts in the lunar wake [4, 5, 6, 7] or even extreme values exceeding a few kilovolts during periods when solar disturbances provide an additional source of hot electrons [8]. Finally, we note that the analyses presented in the Lunar

Prospector papers confine their results to the potential of the lunar surface and no attempt is made to evaluate the charging properties of the spacecraft itself in orbit about the Moon.

Spacecraft charging in lunar environments is not fundamentally different than conditions encountered in previous missions within the Earth's magnetosphere and in the near Earth interplanetary space. The renewed interest in lunar exploration and a return of humans to the Moon however places a particular emphasis on designing safe and reliable systems for operations under a variety of charging conditions. Many of the spacecraft charging tool sets currently in use for evaluating potential distributions and electric fields on the surface and in the space surrounding a spacecraft focus on low Earth orbit (including auroral charging), geostationary orbit, and interplanetary space where the majority of space vehicles are located. It is important to understand if these tool sets are adequate to describe the low density, high temperature environments of the lunar wake as well as the variety of conditions experienced by a spacecraft in lunar orbit while the Moon transits the Earth's magnetotail.

This paper presents Nascap (NASA and Air Force Charging Analyzer Program) -2k [9] surface charging analyses for a candidate lunar orbiting spacecraft to determine if the current version of the Nascap-2k 3-D charging analysis model is adequate for use in designing unmanned lunar orbiting spacecraft and the transportation systems required for human missions to the Moon. The current default Nascap-2k options for computing spacecraft potentials include interplanetary, geostationary, and low Earth orbit environments. Since there is no lunar specific option, we use both the interplanetary and geostationary orbit options here for computing spacecraft surface potentials and electric fields for a range of environments from solar wind, magnetosheath, and into the Earth's magnetotail. Discussion of the results include an assesment of which of the existing options in Nascap-2k provide the most applicable results for lunar applications and what modifications would be desirable to support the analyses required to design space systems for upcoming NASA missiosn to the Moon.

2 - MODEL

A sample model for the Lunar Prospector was written in Object Tool Kit (OTK), the object editing module of Nascap–2k. Figure 1b shows the completed OTK Lunar Prospector model based on an artist rendition of the vehicle given in Figure 1a. Care was taken to represent as acuarately as possible the actual Lunar Prospector spacecraft geometry, however, there is no expectation given that all materials and dimensions are correct. The body of the Nascap-2k spacecraft (cylinder) is covered in solar cells. The top and bottom of the body is covered in graphite. There are three booms extending radially outward from the body. For Nascap-2k purposes, they have been modeled as graphite. At the end of each boom are the science modules. Referring to Figure 1b, the alpha particle spectrometer is represented as the square module in the lower right hand corner of the image. It is modeled as graphite with aluminum square patched on all sides except the side connecting to the boom. The cylinders extending outward from the alpha particle spectrometer are the neutron spectrometers: one is shown as tin and the other as cadmium. The gamma ray spectrometer is extending back on the right side of the image. It is modeled as graphite. The electron reflectometer is attached to the boom extending to the back and left in Figure 1b. The magnetometer is then attached to it via another boom. Both the electron reflectometer and the magnetometer are modeled as graphite. For simplicity, tin and cadmium were created with the same default Nascap-2k properties as aluminum. All remaining materials also use the Nascap-2k default properties.

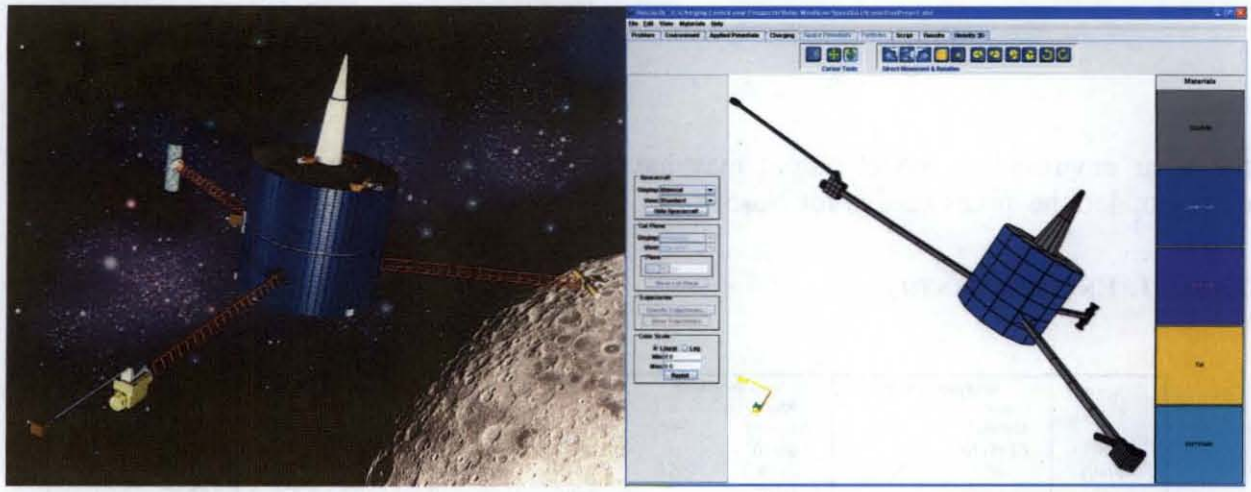

a. b.

Figure 1 - (a) Artist's rendition of the Lunar Prospector spacecraft showing spacecraft bus covered with solar arrays and booms for instrumentation (image courtesy http://nssdc.gsfc.nasa.gov/planetary/lunarprosp.html). (b) Nascap-2k Object Tool Kit model of the Lunar Prospector spacecraft with surface materials adopted for charging analysis indicated by the color scheme including graphite (grey), solar cells (dark blue), cadmium (purple), tin (yellow) and aluminum (light blue).

3 - ENVIRONMENT

The Moon spends approximately 25% of the time inside the Earth's magnetosheath and magnetotail, with the rest of the time spent inside the solar wind. The Moon has no appreciable atmosphere and no global magnetic field, so the charged particles comprising the solar wind, magnetosheath, and magnetosphere interact directly with the lunar surface. Plasma flows produce a plasma wake on the downstream side of the Moon where density depletions within the wake of some two to three orders of magnitude are observed [7]. The first observations of the lunar wake were made by Explorer 35 and the Apollo sub-satellites [10]. There have been a number of more recent observations with spacecraft such as WIND [11] during lunar fly-by maneuvers and Lunar Prospector [7] in low lunar orbit.

In order to estimate charging conditions within the wake, plasma environment parameters relevant for the wake conditions are required for input to the Nascap-2k charging model. We use an analytical model of the wake plasma density and temperature environments for specifying the charging environments in the lunar wake. The wake model is based on functions describing plasma density and temperature variations as a function of depth into the lunar wake and distance from the Moon derived by *Halekas et al.* [7] from Lunar Prospector electron temperature and density observations and model ion environments derived by *Samir et al.* [12]. Based on the ambient solar wind or magnetotail plasma environment, the model calculates the disturbed density and temperature in the wake region for electrons, protons, and alpha particles.

Free-field (upstream) input parameters for the wake model were taken from Paterson and Frank [13] and Feldman et al. [14] for the magnetotail boundary layers, Feldman et al. [14] for the magetosheath, Craven [15] and Feldman et al. [14] for the plasma sheet, and from Newbury et al. [16] and Feldman et al. [14] for the high and low speed solar wind environments. The wake model then provides the plasma conditions at 100 km altitude in the deep lunar wake. Environments given in Table 1 represent the model results for the deep lunar wake which are used as the Nascap-2k input parameters for both interplanetary and geosynchronous (GEO) runs. Slight modifications in

the lunar environment model output may have been made to some, but not all parameters to correspond to the inputs needed for Nascap-2k.

TABLE 1. ENVIRONMENTS

	Boundary Layer		Magnetosheath		Plasma Sheet		Solar Wind High Speed		Solar Wind Low Speed	
	Inter-planetary	Geo	Inter-planetary	Geo	Inter-planetary	Geo	Inter-planetary	Geo	Inter-planetary	Geo
ρ (m^{-3})	7.326×10^{4}		6.64×10^{5}		2.428×10^{4}		266.3		6374	
T_e (eV)	156.7	156.7	290.9	290.9	1316	1316	78.28	78.28	47.78	47.78
v_i (m/s)	5.4×10^{4}		4×10^{5}		2×10^{5}		7.02×10^{5}		3.27×10^{5}	
E_i (eV)	15.22		835.3		208.8		2573		558.2	
ρ_e (m^{-3})		7.326×10^{4}		6.64×10^{5}		2.428×10^{4}		266.3		6374
ρ_i (m^{-3})		6.684×10^{4}		6.06×10^{5}		2.215×10^{4}		50		50
T_i (eV)		111.6		920		995.7		10		10
I_e (A/m^2)	2.458×10^{-8}	2.458×10^{-8}	3.036×10^{-7}	3.036×10^{-7}	2.361×10^{-8}	2.361×10^{-8}	6.316×10^{-11}	6.316×10^{-11}	1.181×10^{-9}	1.181×10^{-9}
I_i (A/m^2)	6.338×10^{-10}	4.416×10^{-10}	4.255×10^{-8}	1.15×10^{-8}	7.779×10^{-10}	4.372×10^{-10}	2.995×10^{-11}	9.891×10^{-14}	3.339×10^{-10}	9.891×10^{-14}
Charging time	300 sec.	300 sec	1000 sec	300 sec	1000 sec	300 sec	1000 sec	300 sec	1000 sec	300 sec

4 - RESULTS

The following subsections describe the results of the Nascap-2k interplanetary and geosynchronous runs for boundary layer, magnetosphere, plasma sheet, high speed solar wind, and low speed solar wind environments. The problem type is a surface charging analysis using analytic currents. All runs were for at least 300 seconds of charging time, with no grid, no magnetic field or sun, an initial electron particle species, and an initial applied potential of -5 volts.

4.1 - BOUNDARY LAYER

Figure 2 shows the potential results of the interplanetary and geosynchronous runs for the boundary layer calculations. Potential results were exactly the same in both runs : 1.60 to 2.90 volts, with the solar cells at 2.90 volts and the graphite areas of the spacecraft at 1.6 volts. For the potential results the interplanetary and geosynchronous runs went to equilibrium immediately and stayed smooth. However, the charging current and electric field results had numerical noise for the geosynchronous run. Interestingly, when plotting the electric field for the interplanetary run, results stabilized at zero V/m. However, for the geosynchronous run, the electric field was between -350 and 400 V/m.

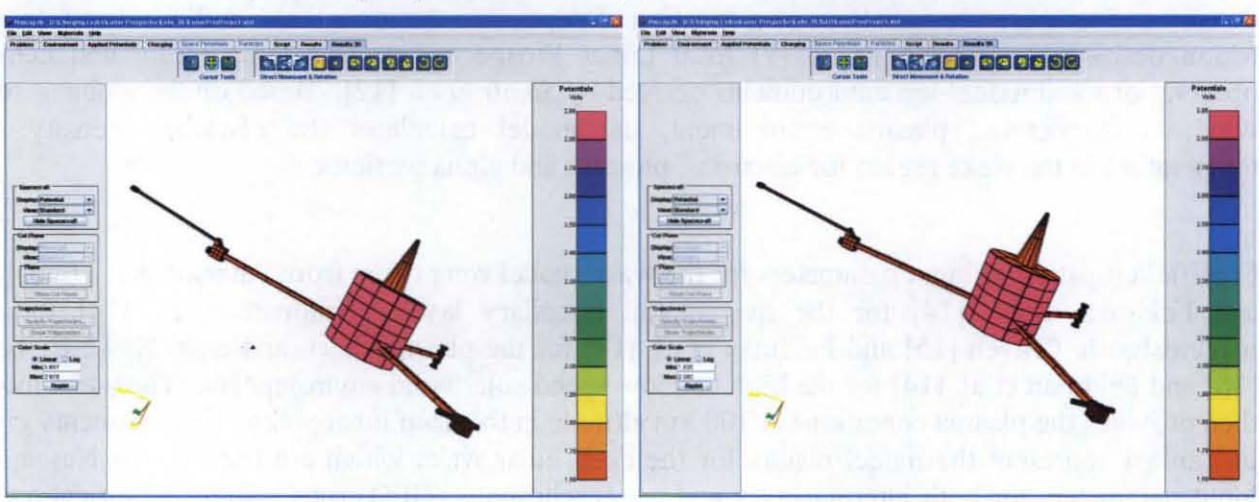

a. b.

Figure 2 - Nascap-2k boundary layer environment potential results using the (a) interplanetary and (b) geosynchronous potential computation options.

4.2 - MAGNETOSHEATH

Figure 3 shows the potential results of the interplanetary and geosynchronous runs for the magnetosheath. Potential results were slightly different for each run : 1.60 to 4.80 volts for the interplanetary run and 1.0 to 3.4 volts for the GEO run. The solar cells showed more variation in end results in the interplanetary run than the GEO run. Again, graphite charged lower than the solar cells for both cases. For the potential results the interplanetary and geosynchronous runs went to equilibrium immediately and stayed smooth. However, the charging current and electric field results for both had small numerical noise. When plotting the electric field for the interplanetary run, results stabilized at zero V/m. However, for the geosynchronous run, the electric field was between -150 and 400 V/m.

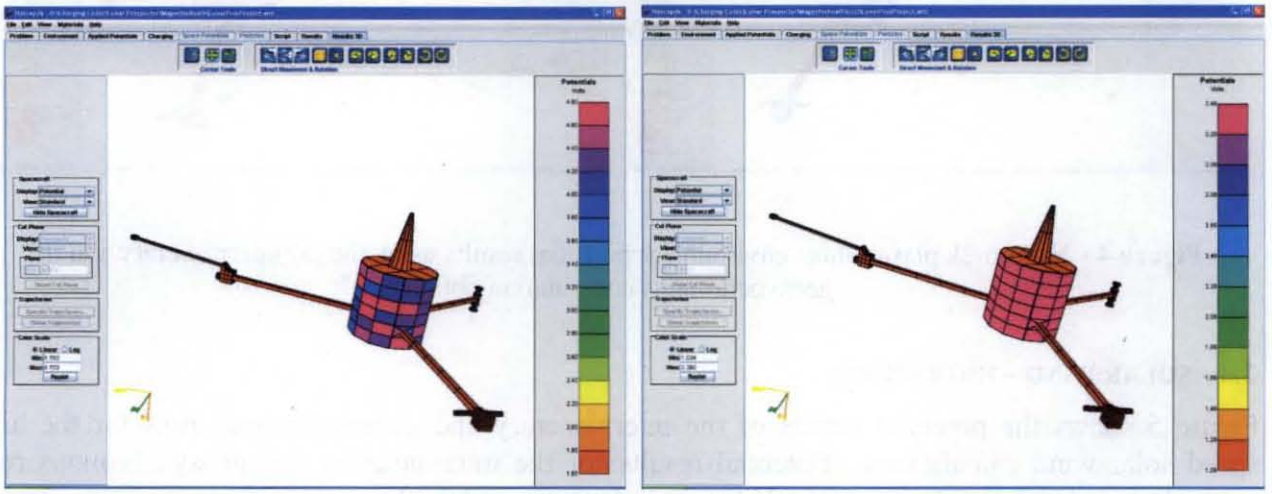

a. b.

Figure 3 - Nascap-2k magnetosheath environment potential results using the (a) interplanetary and (b) geosynchronous computation options.

4.3 - PLASMASHEET

Figure 4 shows the potential results of the interplanetary and geosynchronous runs for the plasmasheet calculations. Potential results were -2.5 to 3.5 V for the interplanetary run and -1.5 to 3.0 V for the GEO run. Again, the solar cells for the interplanetary run showed more variation in charging. Graphite again was more negative. For the potential results the interplanetary run went to equilibrium immediately and stayed smooth, while the GEO run had a sizable amount of numberical noise around equilibrium. There was a small amount of noise for the charging current for both types of runs. The electric field for the GEO run was very noisy around the minimum and maximum values. When plotting the electric field for the interplanetary run, results stabilized at zero V/m. However, for the geosynchronous run, the electric field was between -800 and 800 V/m.

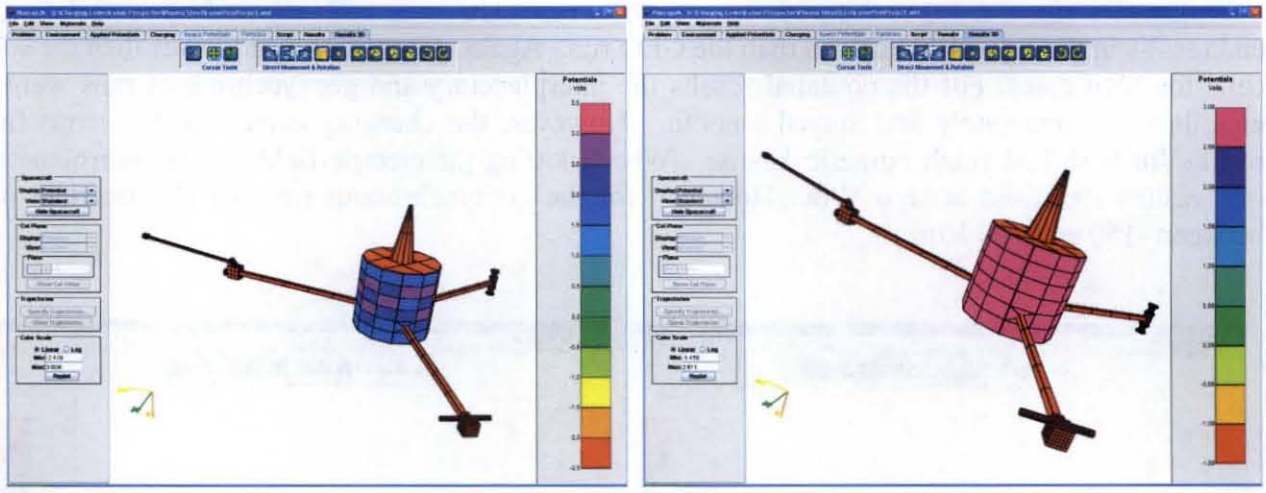

a. b.

Figure 4 - Nascap-2k plasmasheet environment potential results using the (a) interplanetary and (b) geosynchronous computation option.

4.4 - SOLAR WIND – HIGH SPEED

Figure 5 shows the potential results of the interplanetary and geosynchronous runs for the high speed solar wind calculations. Potential results for the interplanetary and geosynchronous runs were almost identical at 0.78 to 0.81 V for interplanetary and 0.79 to 0.80 V for geo. Both went to equilibrium almost immediately and were smooth. The solar cells charged more positive than the graphite for both cases. The charging current and electric field were the same for both with the electric field between -200 and 250 V/m.

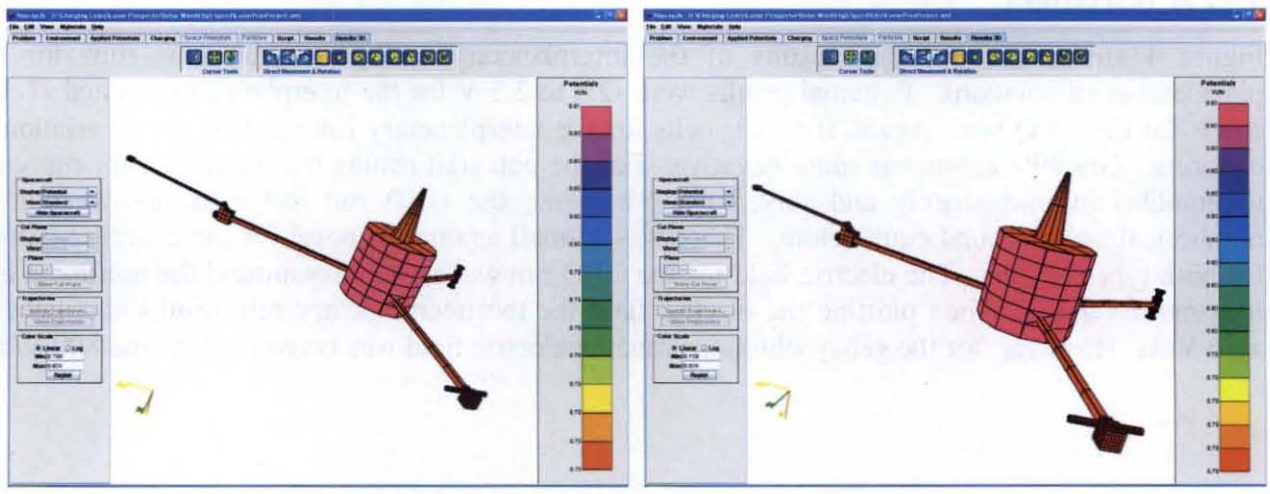

a. b.

Figure 5 - Nascap-2k high speed solar wind environment potential results using the (a) interplanetary and (b) geosynchronous computation option.

4.5 - SOLAR WIND – LOW SPEED

The low speed solar wind case had the largest negative charging of any of the cases ran. Figure 6 shows results from the interplanetary and GEO runs. However, there was basically no differential charging. The interplanetary run produced a potential of -235.6 V, while the GEO run was -154 to -153.9 V. The potential, charging current, and electric field profiles for both interplanetary and

GEO runs were smooth and went to equilibrium within the final charging time. The electric field for the interplanetary case was $-8x10^4$ to $6x10^4$ V/m. The eletric field (**E**-field) for the GEO case was $-5x10^4$ to $4x10^4$ V/m.

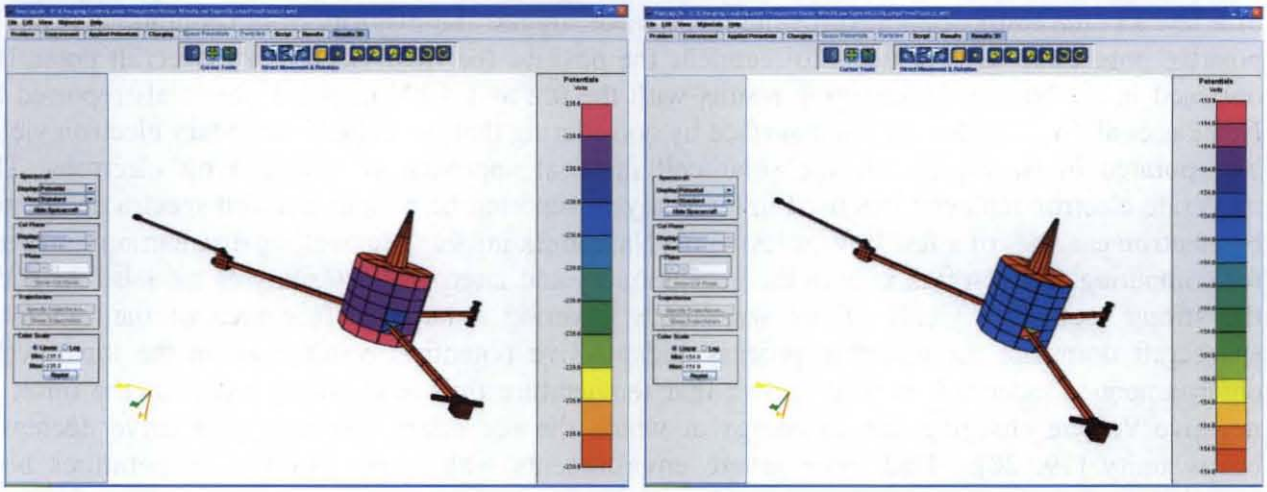

a. b.

Figure 6 - Nascap-2k low speed solar wind environment potential results using the (a) interplanetary and (b) geosynchronous computation option.

Nascap-2k results for all the environments for both interplanetary and geosynchronous runs are summarized in Table 2.

TABLE 2. CHARGING RESULTS

	Boundary Layer		Magnetosheath		Plasma Sheet		Solar Wind High Speed		Solar Wind Low Speed	
	Inter-planetary	Geo	Inter-planetary	Geo	Inter-planetary	Geo	Inter-planetary	Geo	Inter-planetary	Geo
Φ (V) equil.	1.60 to 2.90 immed	1.6 to 2.9 noise ~2V	1.6 to 4.80 immed	1 to 3.4 small noise	-2.5 to 3.5 immed	-1.5 to 3 very noisey	0.78 to 0.81 immed	0.79 to 0.8 immed	-235.6 to equil	-154 to -153.9 to equil
E (V/m)	~0	-350 to 400	~0	-150 to 400	~0	-800 to 800 min and max very noisey	-200 to 250	-200 to 250	-8x104 to 6x104	-5x104 to 4x104
equil.		noise		small noise			immed	immed	to equil	to equil
Charging Current (A/m^2)	-1.2x10-6 to 1.2x10-6	-1.2x10-6 to 1.2x10-6	-1.2x10-6 to 1.2x10-6	-1.0x10-6 to 1.2x10-6	-1.2x10-6 to 1.2x10-6	-1.2x10-6 to 1.2x10-6	-1.1x10-6 to 1.1x10-6	-1.1x10-6 to 1.1x10-6	-1.1x10-6 to 1.1x10-6	-1.1x10-6 to 1.1x10-6
equil.		noise ~0	small noise ~0	tiny noise ~0		tiny noise	immed	immed	to equil	to equil
Charging time	300 sec.	300 sec	1000 sec	300 sec	1000 sec	300 sec	1000 sec	300 sec	1000 sec	300 sec

5 - CONCLUSION

Differences in potentials which result from using the interplanetary and geosynchronous orbit computational options are likely due to how Nascap-2k treats the plasma current for interplanetary problem types as opposed to geosynchronous problem types [Mandell et al.,] since the computational techniques are similar for the both, due to both having a long Debye length and tenuous plasma, except for the plasma current treatment.

While the rule of thumb for charging in darkness is that a vehicle will reach an equilibrium potential of a few kT, the results obtained for the lunar wake suggest the majority of the conditions result in positive potentials. It is possible to reconcile the positive (or small negative) spacecraft potentials obtained in the Nascap-2k charging results with the 0.2 to 1.4 kV negative potentials reported by Halekas et al. [6, 7, 8] for the lunar surface by considering that the default secondary electron yields incorporated in Nascap-2k for the solar cell material approach six for kilovolt electrons. The moderate electron temperatures used in the analyses reported here yield electron spectra dominated by electron energies of a few keV or less since Nascap-2k utilizes Maxwellian distribution functions for computing electron flux in both the geostationary and interplanetary analyses models. As such, the strong secondary yields of the solar cells covering a large surface area of the candidate spacecraft dominate the charging process and positive potentials result even in the lunar wake environments. Indeed, it is well known that temperature threshold effects exist for the onset of negative vehicle charging due to energy at which the secondary electron yield curve decreases below unity [19, 20]. Had more severe environments with larger electron temperatures been included in the case studies, there would have been more negative potentials resulting from the Nascap-2k charging results.

It is likely the environments measured by the Lunar Prospector spacecraft were better represented by Kappa distribution functions [7] since the electron environments in the deep lunar wake are characterized by energetic electrons preferrentially filling the plasma void ahead of the cold electrons and ions. It is recommended to include options for future versions of the Nascap-2k software to model current collection processes with Kappa functions to evaluate this effect, a feature not available in the current version of the code.

Programs such as NASA's new Constellation lunar program would benefit from modification of the current version of the Nascap-2k surface charging model to include a dedicated lunar charging module which includes non-thermal electron and ion distributions, plasma flow velocities independent of the solar illumination direction, and other effects unique to the lunar environment. However, for spacecraft orbiting the moon, the interplanetary environment charging run does an adequate job in calculating the potentials. The GEO problem type seems to do a better job calculating the electric field however. But the GEO problem type has more numerical noise that may or may not be an issue.

6 - BIBLIOGRAPHY

[1] Manka, R. H., *Plasma and potential at the lunar surface, in Photon and Particle Interations With Surfaces in Space*, edited by R. J. L. Grard, pp. 347– 361, Springer, New York, 1973.

[2] Reasoner, D. L., and W. J. Burke, "Characteristics of the lunar photoelectron layer in the geomagnetic tail," J. Geophys. Res., 77, 6671– 6687, 1972.

[3] Freeman J. and M. Ibrahim, *Lunar electric fields, surface potential and associated plasma sheaths*. The Moon 14, 103-114, 1975.

[4] Halekas, J.S., D.L. Mitchell, R.P. Lin, L.L. Hood, M.H. Acuna, and A.B. Binder, "Evidence for negative charging of the lunar surface in shadow," Geophys. Res. Lett., 29, 1435, 2002.

[5] Halekas, J.S., R.P. Lin, and D.L. Mitchell, "Inferring the scale height of the lunar nightside double layer," Geophys. Res. Lett., 30, 2117, 2003.

[6] Halekas, J.S., R.P. Lin, and D.L. Mitchell, "Large negative lunar surface potentials in sunlight and shadow," Geophys. Res. Lett., 32, 9102, 2005a.

[7] Halekas, J.S., S.D. Bale, D.L. Mitchell, and R.P. Lin, "Electrons and magnetic fields in the lunar plasma wake," J. Geophys. Res., 110, 7222, 2005b.

[8] Halekas, J.S., G.T. Delory, D.A. Brain, R.P. Lin, M.O. Fillingim, C.O. Lee, R.A. Mewaldt, T.J. Stubbs, W.M. Farrell, and M.K. Hudson, "Extreme lunar surface charging during solar energetic particle events," Geophys. Res., Lett., 34, 2111, 2007.

[9] Mandell, M. J., V. A. Davis, B. M. Gardner, I. G. Mikellides, D. L. Cooke, J. Minor, "NASCAP-2K, An Overview," 8th Spacecraft Charging and Technology Conference, Huntsville, AL, 2003.

[10] Schubert, G., and R. B. Lichenstein, Observations of Moon-plasma interactions by orbital and surface experiments, *Rev. Geophys., 12*, 592-626, 1974.

[11] Olgilvie, K. W., J. T. Steinberg, R. L. Fitzenreiter, C. J. Owen, A. J. Lazarus, W. M. Farrell, and R. B. Torbert, Observations of the lunar plasma wake from the WIND spacecraft on December 27, 1994, *J. Geophys. Res. Lett., 23*, 1255-1258, 1996.

[12] Samir, U., K. H. Wright Jr., and N. H. Stone, "The expansion of a plasma into a vacuum: Basic phenomena and processes and applications to space plasma physics," Rev. Geophys., 21, 1631-1646, 1983.

[13] Paterson, W.R., and L.A. Frank, "Survey of plasma parameters in Earth's distant magnetotail with the Geotail spacecraft," Geophys. Res. Lett., 21, 2971 – 2974, 1994.

[14] Feldman W.C., J.R. Asbridge, S.J. Bame, and J.T. Gosling, Plasma and Magnetic Fields from the Sun, in *The Solar Output and its Variation*, (ed.) Oran R. White, Colorado Associated University Press, Boulder, 1977.

[15] Craven, T.E., *Physics of Solar System Plasmas*, Cambridge University Press, 1997.

[16] Newbury, J.A., C.T. Russell, J.L. Phillips, and S.P. Gary, "Electron temperature in the ambient solar wind: typical properties and a lower bound at 1 AU," JGR, 103, 9553 – 9566, 1998.

[17] Mandell, M. J., I. Katz, J. M. Hilton, D. L. Cooke, and J. Minor, "Nascap-2k Spacecraft Charging Models: Algorithms and Applications," 7th Spacecraft Charging and Technology Conference, Noordwijk, The Netherlands, 2001.

[18] Olsen, R.C., "A threshold effect for spacecraft charging," J. Geophys. Res., 88, 493 - 499, 1983

[19] Lai, S.T. and M.F. Tautz, "Aspects of spacecraft charging in sunlight," IEEE Trans. Plasma Sci., 34, 2053 - 2061, 2006.

MSFC-191 — PRESENTATION

Analysis of Lunar Surface Charging for a Candidate Spacecraft Using Nascap-2k

Linda Neergaard Parker
Jacobs, ESTS Group

Joseph I. Minow
NASA, Marshall Space Flight Center

William C. Blackwell
Jacobs, ESTS Group

Abstract

The characterization of the electromagnetic interaction for a spacecraft in the lunar environment, and identification of viable charging mitigation strategies, is a critical lunar mission design task, as spacecraft charging has important implications both for science applications and for astronaut safety. To that end, we have performed surface charging calculations of a candidate lunar spacecraft for lunar orbiting and lunar landing missions. We construct a model of the spacecraft with candidate materials having appropriate electrical properties using Object Toolkit and perform the spacecraft charging analysis using Nascap-2k, the NASA/AFRL sponsored spacecraft charging analysis tool. We use nominal and atypical lunar environments appropriate for lunar orbiting and lunar landing missions to establish current collection of lunar ions and electrons. In addition, we include a geostationary orbit case to demonstrate a bounding example of extreme (negative) charging of a lunar spacecraft in the geostationary orbit environment. Results from the charging analysis demonstrate that minimal differential potentials (and resulting threat of electrostatic discharge) occur when the spacecraft is constructed entirely of conducting materials, as expected. We compare charging results to data taken during previous lunar orbiting or lunar flyby spacecraft missions.

Lunar Prospector Model

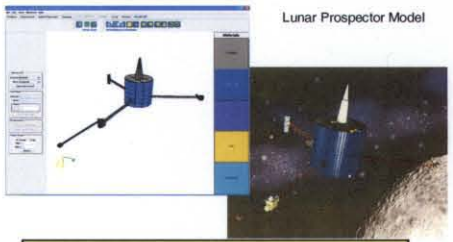

1a. Nascap-2k Object Tool Kit model of Lunar Prospector and 1b. Image of Lunar Prospector taken from NASA image ????? or http://www.lpi.usra.edu/expmoon/prospector/prospector.html

Lunar Wake Charging

The Moon spends about 25% of the time inside the Earth's magnetosheath, with the rest of the time spent inside the solar wind. The Moon has no appreciable atmosphere and no global magnetic field, so the charged particles comprising the solar wind, magnetosheath, and magnetosphere interact directly with the lunar surface, leaving a plasma wake of decreased density [*Halekas et al.*, 2005]. The first observations of the lunar wake were made by Explorer 35 and the Apollo sub-satellites [*Schubert and Lichenstein*, 1974]. There have been a number of more recent observations with spacecraft such as WIND [*Olgilvie et al.*, 1996] and Lunar Prospector [*Halekas et al.*, 2005].

Lunar Wake Model

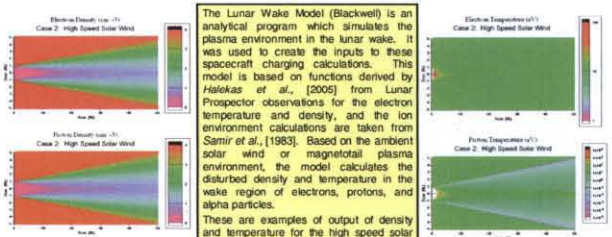

The Lunar Wake Model (Blackwell) is an analytical program which simulates the plasma environment in the lunar wake. It was used to create the inputs to these spacecraft charging calculations. This model is based on functions derived by *Halekas et al.*, [2005] from Lunar Prospector observations for the electron temperature and density, and the ion environment calculations are taken from *Samir et al.*, [1983]. Based on the ambient solar wind or magnetotail plasma environment, the model calculates the disturbed density and temperature in the wake region of electrons, protons, and alpha particles.

These are examples of output of density and temperature for the high speed solar wind case.

Charging Environments for Nascap-2k Analysis

	Boundary Layer		Magnetosheath		Plasma Sheet		Solar Wind High Speed		Solar Wind Low Speed	
	Inter-planetary	Geo	Inter-planetary	Geo	Inter-planetary	Geo	Inter-planetary	Geo	Inter-planetary	Geo
n (m^{-3})	7.326×10^{6}		6.64×10^{6}		2.43×10^{6}		26.3		0374	
T_e (eV)	136.7	136.7	295.8	295.8	1316	1316	76.28	76.28	47.79	47.79
v (m/s)	6.4×10^{5}		4.66×10^{5}		2.27×10^{5}		7.62×10^{5}		2.27×10^{5}	
Φ (eV)	-15.70		895.5		3599		3573		558.3	
n (m^{-3})		7.326×10^{6}		6.64×10^{6}		2.43×10^{6}		26.3		0374
n (m^{-3})		6.684×10^{6}		6.66×10^{6}		2.215×10^{6}		59		59
T_i (eV)		111.6		600		3265.7		19		19
v_{th} (m/s)	2.468×10^{6}	2.468×10^{6}	3.098×10^{6}	3.098×10^{6}	2.381×10^{6}	2.381×10^{6}	5.354×10^{5}	5.354×10^{5}	1.181×10^{6}	1.181×10^{6}
j_{ram} (A/m^2)	5.888×10^{-9} 3000 sec	4.414×10^{-9} 900 sec	4.203×10^{-9} 1000 sec	1.15×10^{-9} 300 sec	7.779×10^{-9} 1000 sec	4.972×10^{-9} 300 sec	2.868×10^{-9} 1000 sec	2.868×10^{-9} 300 sec	8.606×10^{-9} 1000 sec	8.961×10^{-9} 300 sec

Feldman, et al., *Plasma and Magnetic Fields From the Sun,In the Solar Output and Its Variation*, Table 4, 1977.

Craven, T.E., *Physics of Solar System Plasmas*, Cambridge University Press, 1997.

Paterson, W.R., and L.A. Frank, "Survey of plasma parameters in Earth's distant magnetotail with the Geotail spacecraft," Geophys. Res. Lett., 21, 2971-2974, 1994.

Newbury, J.A., C.T. Russell, J.L. Phillips, and S.P. Gary, "Electron temperature in the ambient solar wind:typical properties and a lower bound at 1 AU," JGR, 103, 9553-9566, 1998.

Magnetosheath Environment Results

Interplanetary module results | Geosynchronous module results

Interplanetary Results

Spacecraft Solar Arrays$_{ave}$: 4.236 V
Booms: 1.762 V
Alpha particle detector: 1.762 V
Neutron Spectrometer: 1.762 V
Gamma Ray Spectrometer: 1.762 V
Electron Reflectometer: 1.762 V
Magnetometer: 1.762 V
Sunlight$_{ave}$: 1.802 V
Eclipse$_{ave}$: 3.110

Plasmasheet Environment Results

Interplanetary module results | Geosynchronous module results

Interplanetary Results

Spacecraft Solar Arrays$_{ave}$: 2.109 V
Booms: -2.478 V
Alpha particle detector: -2.478 V
Neutron Spectrometer: -2.478 V
Gamma Ray Spectrometer: -2.478 V
Electron Reflectometer: -2.478 V
Magnetometer: -2.478 V
Sunlight$_{ave}$: -2.405 V
Eclipse$_{ave}$: 0.2163 V

Low Speed Solar Wind Environment Results

Interplanetary module results | Geosynchronous module results

Interplanetary Results

Spacecraft Solar Arrays$_{ave}$: -235.6 V
Booms: -235.6 V
Alpha particle detector: -235.6 V
Neutron Spectrometer: -235.6 V
Gamma Ray Spectrometer: -235.6 V
Electron Reflectometer: -235.6 V
Magnetometer: -235.6 V
Sunlight$_{ave}$: -235.6 V
Eclipse$_{ave}$: -235.6 V

Recommendations for Future Work

It is recommended to include options for future versions of the Nascap-2k software to model current collection processes with Kappa functions to evaluate this effect, a feature not available in the current version of the code.

Programs such as NASA's new Constellation lunar program would benefit from modification of the current version of the Nascap-2k surface charging model to include a dedicated lunar charging module which includes

- non-thermal electron and ion distributions,
- plasma flow velocities independent of the solar illumination direction,
- and other effects unique to the lunar environment.

Summary of Surface Potentials

	Boundary Layer		Magnetosheath		Plasma Sheet		Solar Wind High Speed		Solar Wind Low Speed	
	Inter-planetary	Geo	Inter-planetary	Geo	Inter-planetary	Geo	Inter-planetary	Geo	Inter-planetary	Geo
Φ (V) equil.	1.60 to 2.90 immed	1.6 to 2.9 noise -2V	1.6 to 4.80 immed	1 to 3.4 small noise	-0.5 to 3.5 immed	-1.5 to 3 very noisey	0.78 to 0.81 immed	0.78 to 0.8 immed	-235.6 to equil -9x104 to 4x104	-153.9 to equil -9x104 to 4x104
E (V/m) equil.	~0	-350 to 400 noise	~0	-150 to 400 small noise	~0	-800 to 800 min and max very noisey	-200 to 250 immed	-200 to 250 immed	to equil	to equil
Charging Current (A/m^2) equil.	-1.2x10-6 to 1.2x10-6	-1.2x10-6 to 1.2x10-6 noise ~0	-1.2x10-6 to 1.2x10-6 small noise ~0	-1.0x10-6 to 1.2x10-6 tiny noise ~0	-1.2x10-6 to 1.2x10-6 tiny noise	-1.2x10-6 to 1.2x10-6 tiny noise	-1.1x10-6 to 1.1x10-6 immed	-1.1x10-6 to 1.1x10-6 immed	-1.1x10-6 to 1.1x10-6 to equil	-1.1x10-6 to 1.1x10-6 to equil
Charging time	300 sec	300 sec	1000 sec	300 sec	1000 sec	300 sec	1000 sec	300 sec	1000 sec	300 sec

Conclusions

While the rule of thumb for charging in darkness is a vehicle will reach an equilibrium potential of a few kV, the results obtained for the lunar wake suggest the majority of the conditions result in positive potentials. It is possible to reconcile the positive (or small negative) spacecraft potentials obtained in the Nascap-2k charging results with the 0.2 to 1.4 kV negative potentials reported by Halekas et al. [2005a,b; 2007] for the lunar surface by considering that the default secondary electron yields incorporated in Nascap-2k for the solar cell material approach 8 for kilovolt electrons. The moderate electron temperatures used in the analyses reported here yield electron spectra dominated by electron energies of a few keV or less since Nascap-2k utilizes Maxwellian distribution functions for computing electron flux. In both the geostationary and interplanetary analyses models. As such, the strong secondary yields of the solar cells covering a large surface area of the candidate spacecraft dominate the charging process and positive potentials result even in the lunar wake environments. Indeed, it is well known that temperature threshold effects exist for the onset of negative vehicle charging due to energy at which the secondary electron yield curve decreases below unity [Olsen, 1983; Lai et al. 2003]. Had more severe environments with larger electron temperatures been included in the case studies, there would have been more negative potentials resulting from the Nascap-2k charging results.

It is likely the environments measured by the Lunar Prospector spacecraft were better represented by Kappa distribution functions [Halekas et al., 2005b] since the electron environments in the deep lunar wake are characterized by energetic electrons preferentially filling the plasma void ahead of the cold electrons and ions. It is recommended to include options for future versions of the Nascap-2k software to model current collection processes with Kappa functions to evaluate this effect, a feature